Polyhedron Vol. 9, No. 15/16, pp. 1901–1911, 1990
Printed in Great Britain

0277-5387/90 $3.00 + .00

THE KAGOMÉ NET: BAND THEORETICAL AND TOPOLOGICAL ASPECTS*

ROY L. JOHNSTON† and ROALD HOFFMANN‡

Department of Chemistry and Materials Science Center, Cornell University, Ithaca, NY 14853, U.S.A.

Abstract—The Kagomé net (a two-dimensional hexagonal network comprising triangles and hexagons) is a building block of a number of intermetallic compounds. In order to understand the electronic characteristics of such an array of atoms, extended Hückel tight binding calculations have been performed on a Kagomé net of boron atoms. Comparisons have been drawn with other hexagonal nets, namely the graphite net and the close packed triangular net, and topological relationships between these nets are used to explain similarities in their band spectra. It is shown that simple Hückel theory can be used to obtain a rough estimate for the energies of the bands at specific high symmetry k-points, and a way of representing and evaluating energies of crystal orbitals with complex coefficients is discussed. A moments-based analysis of the relative energies of the three nets as a function of electron count is also presented. The effect on its band structure of trigonally distorting the Kagomé net is investigated. Finally, substituted ABC and AB_2 derivatives of the Kagomé net are discussed.

A particularly useful way of describing complex solids is via a conceptual decomposition of the structure into layers and nets.[1] This paper deals with a planar net (the so-called Kagomé net)[1a] which is found in a number of complex intermetallic compounds, most notably the Laves phases ($MgCu_2$, $MgZn_2$ and $MgNi_2$ types).[2] The Laves phases, which possess interesting electronic and magnetic properties[3] as well as being of great interest from a structural point of view,[2a,4] are the subject of a separate publication.[5]

The Kagomé net (**1**) is four-connected (each vertex has four neighbours) and is described by the indices (3636), meaning that if we start counting the rings around any vertex from one of the triangles we encounter in order (independent of the direction of motion) a triangle followed by a hexagon, then another triangle and finally another hexagon.[1a] It is a hexagonal net, belonging to the plane group *p6mm*.[6] The dashed line in **1** denotes the primitive unit cell of the net.

More familiar two-dimensional hexagonal nets are the graphitic (6^3) net (**2**), and the triangular or close packed (3^6) net (**3**).

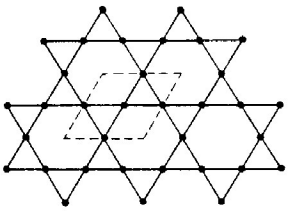

1

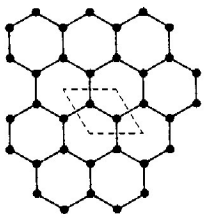

2

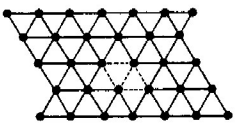

3

In the following sections we shall investigate the electronic band spectrum characteristic of a Kagomé net of main group atoms (boron), making comparisons with alternative graphitic and close packed layer structures. Calculations of the extended Hückel[7a] tight binding [7b,c] type were performed. Standard parameters for boron were chosen ($H_{ii}(2s) = -15.2$ eV, $H_{ii}(2p) = -8.5$ eV, $\zeta(2s) = \zeta(2p) = 1.30$).[7d] Average properties were

* This paper is dedicated to Dick Fenske, a scientist who always tries to understand, deeply.

† SERC/NATO Postdoctoral Fellow 1987–1989.

‡ Author to whom correspondence should be addressed.

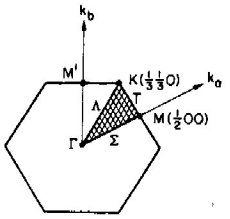

4

calculated using the irreducible wedge of the Brillouin zone shown in **4** (hashed area), with k-points chosen according to the geometrical method of Ramirez and Böhm.[7e]

While there are hundreds of Laves phases, only one of them contains boron. Many more do contain aluminium. And there is no phase in which the Kagomé net forms a separate bonded entity (we are using here the words of a perceptive reviewer of this paper). Why then study this net, for a main group element that does not form it?

The reason is that the net is simple and symmetrical. Stackings of it are plausible. It deserves to be studied; the question, one which will be approached in this paper, is why does it not occur, or, optimistically, what electron counts might favour its materialization.

COMPARISON OF THE BAND STRUCTURES OF KAGOMÉ, GRAPHITIC AND CLOSE PACKED NETS OF BORON ATOMS

In the solid state, boron is known to form icosahedral clusters which are bonded together in a three-dimensional lattice.[8] The connectivity of the boron atoms is six. This should be contrasted with the three-dimensional allotropes of carbon (e.g. diamond) where the carbon atoms are four-connected. It is also well known that boron forms molecular clusters with atom connectivities of five or more,[9] while carbon maintains an approximately tetrahedral local environment.[10] Electron-deficient atoms such as boron (with fewer electrons than valence orbitals) adopt highly-connected structures (with more nearest neighbours than valence orbitals) because such structures are known to stabilize the small number of occupied orbitals to a greater extent.[11] If this idea of increasing connectivity in order to mitigate electron deficiency is carried over into two-dimensions (think of three-connected layers of carbon atoms in graphite) then a layer structure based on Kagomé or close packed nets of boron atoms becomes an interesting possibility. We do not imply that two-dimensional elemental boron nets are likely—boron clearly likes icosahedra. But perhaps formally charged boron sheets of this type might occur in binary AB_x structures.

If we assume constant distances between connected vertices (bearing in mind that for nets of atoms the bond lengths generally increase with connectivity) then the relative densities of the three hexagonal nets (**1**–**3**) discussed above increase in the order graphite (1.0) < Kagomé (1.125) < close packed (1.5). Figure 1 depicts the partial band structures for nets of boron atoms (with B—B bonds of 1.8 Å) with these structures. Unit cells were chosen with one (close packed), two (graphite) and three (Kagomé) atoms (see **1**–**3**).

The Brillouin zone (BZ) has the same symmetry for all three nets (see **4**). Rather than using the plane group *p6mm*, it is convenient to assign these structures to the three-dimensional space group *P6mmm* (D_{6h}^1),[6] since the horizontal mirror plane is a good

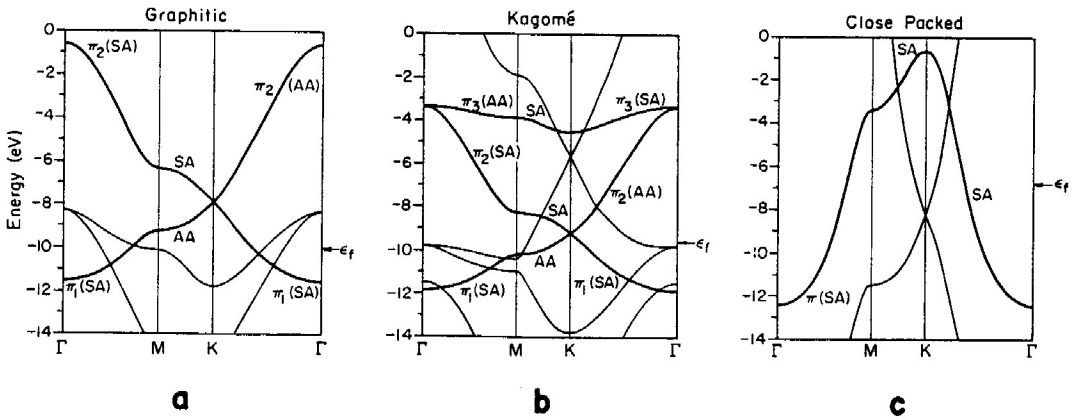

Fig. 1. Band structures of boron with the graphite, Kagomé and close packed (2-d) structures. The π-bands are highlighted and their symmetries with respect to vertical and horizontal mirror planes are indicated.

symmetry element, distinguishing between σ- and π-bands. The symmetries of the special points in the BZ (**4**) (i.e. the "group of k", G_k) for the space group *P6mmm* are as follows: $G_\Gamma = D_{6h}$; $G_M = D_{2h}$; $G_K = D_{3h}$, while the symmetries of the symmetry lines in the BZ are: $G_\Sigma = G_T = G_\Lambda = C_{2v}$.[12] We expect, therefore, to observe degeneracies at Γ and K, but not M. This is indeed the case, as can be seen in Fig. 1. We are only here interested in the π-bands. The labels of the bands (SA and AA) refer to the symmetries of the π bands (S = symmetric, A = antisymmetric) with respect to the two mirror planes containing each of the specified symmetry lines (where the first refers to the vertical plane and the second to the horizontal plane).

From the Figure, it is evident that, for boron, with three valence electrons per atom, all three structures are metallic due to overlap of the σ- and π-bands (the latter have been highlighted). Other interesting features of Fig. 1 include, for Kagomé boron [Fig. 1(b)], the small dispersion of the top π-band (π_3), the non-bonding nature of the middle π-band (π_2) at M (the energy of the atomic boron $2p$ orbitals is -8.5 eV) and the non-bonding nature of the degenerate π-bands at K in the graphite structure [Fig. 1(a)]. We shall endeavour to explain these features in the following paragraphs.

Each of these three planar sheet geometries presents interesting features, which are more or less familiar. The graphite network is best known, the Kagomé net least known. So we will concentrate on the latter.

The π-symmetry crystal orbitals of Kagomé boron (at the high symmetry points Γ, M and K) are sketched in Fig. 2, where the constituent atomic p-orbitals are shown in projection). To understand the figure, however, it will first be necessary to talk a little about the shading conventions used and the problem of the phase angle.

COMPLEX CRYSTAL ORBITALS: PHASE ANGLES AND OVERLAP

We are used to discussing bonding in terms of linear combinations of real atomic orbital functions. In the case of a simple diatomic, such as H_2, the orbital overlap (as a function of internuclear separation, r) is equal to $\pm S(r)$. The overlap is positive (stabilizing) when the orbitals are "in-phase" (**5a**) and negative (destabilizing) when the

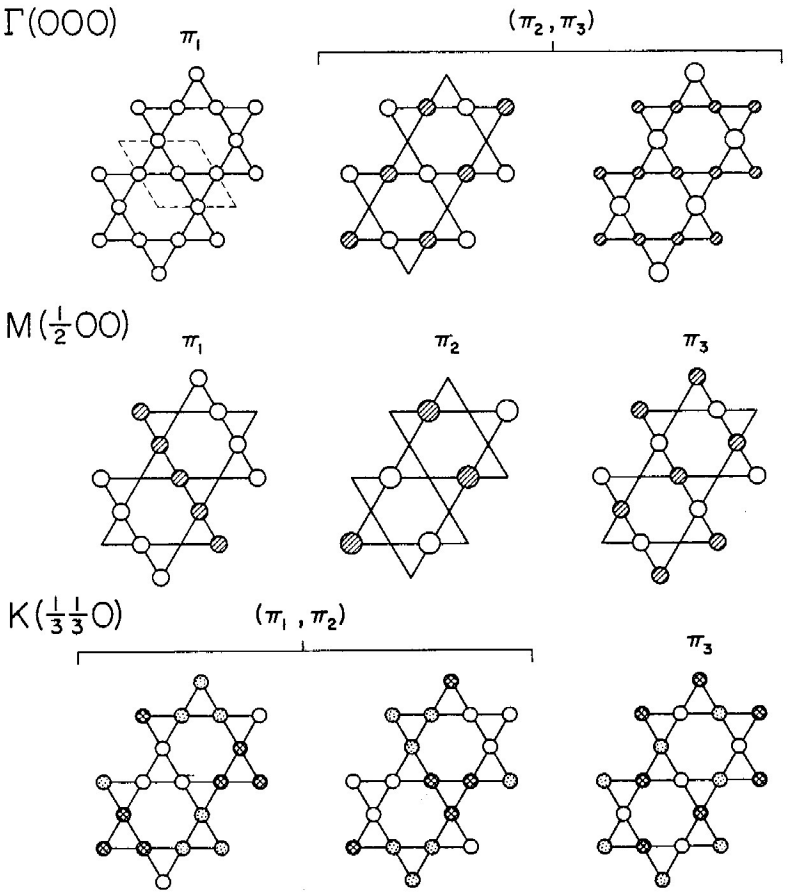

Fig. 2. Representation of the crystal orbitals of Kagomé boron at points Γ, M and K in the BZ.

5a 5b

orbitals are "out-of-phase" (**5b**). In the solid state, however, in most regions of the BZ (including some high symmetry points, such as K in the space group $P6mmm$) the crystal orbitals have coefficients which are complex (of the form $a+ib$, where $i=\sqrt{-1}$) rather than real. By depicting the coefficients of orbitals on neighbouring atoms as vectors on an Argand diagram we can calculate the angles made between these vectors and the (real) positive x-axis. These angles are the absolute "phase angles" (θ) of the orbital. However, in order to determine the size and sign of the overlap between neighbouring orbitals, it is the difference in "phase angle" ($\Delta\theta$) which is important. These concepts are illustrated in **6**, for an example where the coefficients have the same magnitude (i.e. the vectors have the same length, $a^2+b^2=c^2+d^2$).

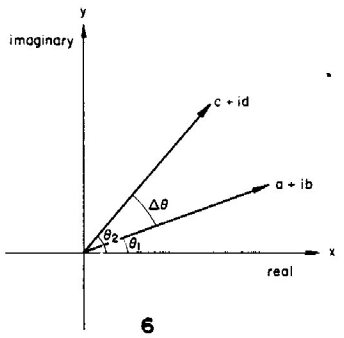

6

As a convention, we generally make one of the coefficients arbitrarily positive and real (i.e. lying along the positive x-axis of the Argand diagram), since only the relative phase angles (i.e. the differences) are important. Classical "in-phase" and "out-of-phase" combinations have phase angle differences ($\Delta\theta$) of 0 and 180°, respectively. The general expression for overlap between a pair of orbitals at separation r, with a phase angle difference of $\Delta\theta°$ between them, is:

$$S_{\Delta\theta}(r) = S_0(r)\cdot\cos(\Delta\theta),$$

where $S_0(r)$ is the overlap integral for $\Delta\theta = 0°$. From this formula, it can readily be seen that, when a pair of complex orbitals are orthogonal ($\Delta\theta = \pm 90°$) the overlap between them is zero.

The crystal orbitals in Fig. 2 have atomic orbital contributions related by factors $e^{2\pi i/3}$, $e^{\pi i}$, $e^{4\pi i/3}$, $e^{2\pi i}$, i.e. relative phase angles of 120, 180, 240 and 360° (≡0°). The shading conventions used to represent these phase angles are shown in **7**. The $\Delta\theta$

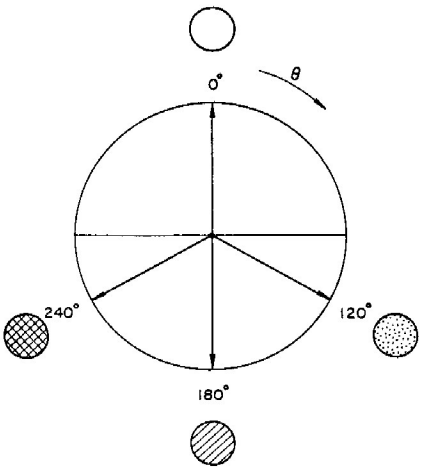

7

values which are present in the crystal orbitals shown in Fig. 2 are: 0 and 180° at Γ and M; and 0, 120 and 240° (−120°) at K. The corresponding overlaps are as follows:

S_0 ("in-phase") at a constant (arbitrary) separation

$S_{180} = -S_0$ ("out-of-phase")

$S_{120} = S_{240} = -0.5S_0$ ("half-out-of-phase").

The ideas developed above can be extended from the calculations of the overlap between complex orbitals to an estimation of their energies by means of simple Hückel theory.[13] Thus, the Hückel resonance energy (β) can be given a phase angle (difference) dependence:

$$\beta_{\Delta\theta} = \beta_0\cdot\cos(\Delta\theta)$$

while the Coulomb energy (α) is independent of phase angle.

It should be noted that the three orbital shadings shown in the representations of the crystal orbitals at K are equally out-of-phase (or in-phase) with respect to each other. This has an important effect which is related to the theory of alternancy.[14] An alternant (two- or three-dimensional) network or graph is one in which all rings or cycles (connected subgraphs) are even-membered. These networks (such as the square lattice shown in **8**) have the

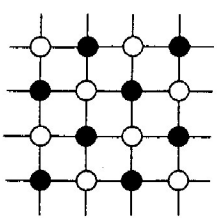

8

property that the vertices can be coloured in one of two ways such that no two adjacent vertices are coloured the same. In terms of atomic lattices, this means that there is always one crystal orbital in which all of the nearest-neighbour interactions are antibonding ($\Delta\theta = 180°$).[15] If we have three different colours (or types of shading) we can extend this principle to (some) systems containing odd-membered rings, such as the Kagomé net, which we shall describe as three-alternant. In three-alternant atomic lattices there will always be a crystal orbital (e.g. π_3 at K in the Kagomé net) in which all nearest-neighbour interactions are equally antibonding, though the phase angle difference ($\Delta\theta$) is now $\pm 120°$.

The small dispersion of the π_3-band in Kagomé boron [Fig. 1(b)] can be explained by examining the crystal orbitals in Fig. 2. At M the π_3-orbital is antibonding along chains of connected boron atoms. In a simple Hückel sense,[13] the energy of this band would be $\alpha - 2\beta$. At Γ the π_3-orbital is one of a degenerate pair, one component of which can also be represented as antibonding chains of borons, with a Hückel energy of $\alpha - 2\beta$. The energies of the bands in our extended Hückel calculation (and in reality) depart from the simple Hückel model through the inclusion of small non-nearest-neighbour interactions. The next-nearest-neighbour interactions at M are overall bonding while those at Γ are net antibonding, so the π_3-band lies at lower energy at M than the π_2/π_3 pair at Γ [see Fig. 1(b)]. At point K in the BZ, as mentioned above, the π_3-band describes a three-alternant pattern. In simple Hückel terms the energy of this crystal orbital would be $\alpha + 4(-0.5\beta) = \alpha - 2\beta$, once more. This time the next-nearest-neighbour interactions are more bonding (each atomic orbital has four next-nearest-neighbour orbitals which are in-phase) than at Γ or M, so the π_3-band shows a minimum at K. Thus, the bonding character of the π_3-band changes very little throughout the BZ. In the density of states (DOS) diagram for this net (not shown here), the flat π_3-band leads to a sharp spike. Because this band is so high above any realistic Fermi level, it is unlikely to have any consequence.

The π_2-band in the Kagomé structure is interesting in that it is antibonding at Γ (where it is degenerate with π_3), non-bonding at M (Hückel energy $= \alpha$), as there are no non-zero coefficients on adjacent sites and bonding at K, where it is degenerate with π_1 (Hückel energy $= \alpha + 2\beta + 2(-0.5\beta) = \alpha + \beta$). From Fig. 1 it can be seen that the π_1-band of graphite at M lies at almost exactly the same energy as the Kagomé π_2-band at K. Indeed the Hückel energy of this orbital (**9a**) is also $\alpha + \beta$. Incidentally, the upper π-band (π_2) of graphite at M (**9b**) is antibonding by the same amount (Hückel energy $= \alpha - \beta$) as π_1 is bonding.[16] As for the Kagomé π_2-band at M, the non-bonding nature of the two degenerate π-bands at K for the graphite structure [Fig. 1(c)] can also be rationalized in terms of complex linear combinations which have nodes at every second atom (**9c**).

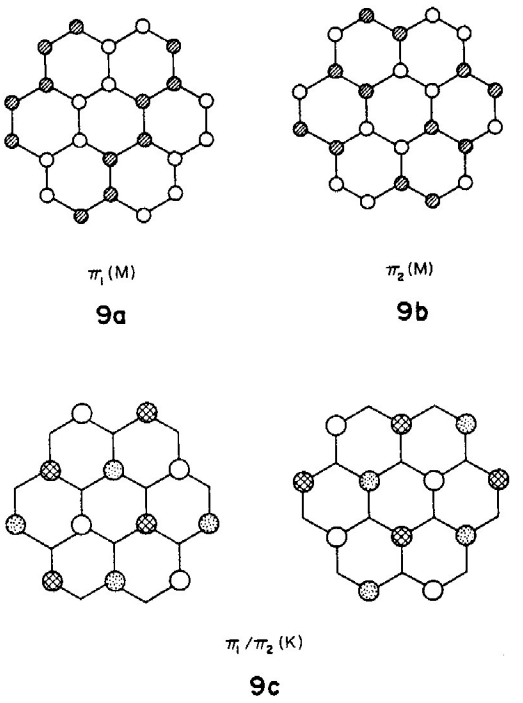

9a **9b** **9c**

From Fig. 1 (a and b), it is apparent that the π_1- and π_2-bands of the Kagomé net exhibit the same pattern as the two π-bands of the graphite net. Figure 3 shows the spectra of crystal orbitals at Γ, M and K for the two structures, with simple Hückel energies given, together with the spectrum of π-MO's obtained for the unit cell contents. It can be seen that at all the high symmetry points of the BZ the Kagomé π_1- and π_2-orbitals are stabilized with respect to those of graphite by β. The reason for this similarity can be traced to the topological relationship which exists between the two nets. Thus, the loci of the centroids of the triangles in the Kagomé net define the graphite net (similarly the centroids of the Kagomé hexagons define the close packed triangular net). The degenerate π-bands of graphite at K (**9c**) can be generated from those of the Kagomé net (Fig. 2) by replacing a triangle (in which all the atomic orbital contributions are in-phase) by a single atomic orbital, with the same phase. Triangles where there are three out-of-phase ($\Delta\theta = 120°$) coefficients are replaced by single atoms with zero atomic orbital coefficients (i.e. nodes).

The single π-band in the close packed structure [Fig. 1(c)] is highly dispersed, due to the high connectivity (six) of the lattice. The minimum energy

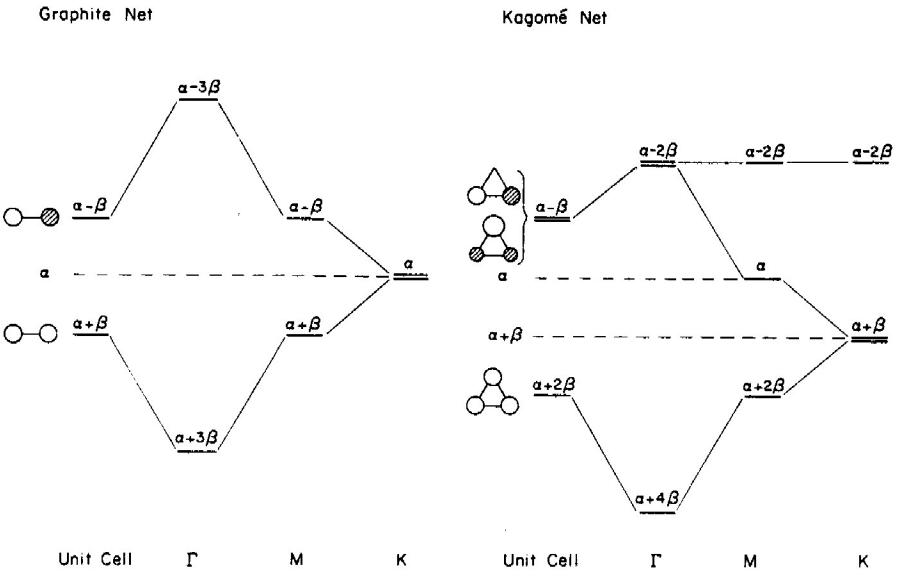

Fig. 3. Comparison of the spectra of crystal orbitals at the high symmetry BZ points for the graphite and Kagomé structures.

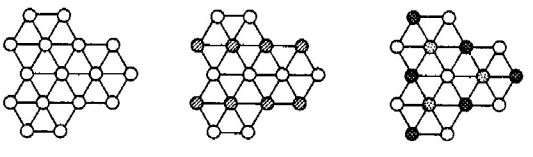

10a **10b** **10c**

occurs at Γ, where each atom experiences a bonding interaction with its six nearest neighbours (**10a**). At M, the π-band (**10b**) has a simple Hückel energy of $\alpha-2\beta$ and, indeed from Fig. 1 it can be seen that the energy of the π-band at M is close to that of the π_3-band of the Kagomé structure. At K, the π-band of the close packed structure has complex coefficients, again with phase angle differences of 0 and $\pm 120°$, and the crystal orbital may once more be represented by a three-alternant colouring (**10c**). The simple Hückel energy of the crystal orbital depicted in **10c** is $\alpha+6(-0.5\beta)=\alpha-3\beta$, which is the same energy as that of the π_2-band of graphite at Γ (**11**), where the connectivity is only three but the neighbouring orbitals are completely (180°) out-of-phase (since graphite is an alternant net).

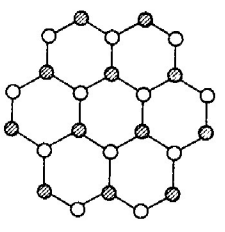

11

Of the two-dimensional structures studied for boron, the graphitic structure is calculated to be the most stable (by 0.47 eV/atom over Kagomé boron and by 1.46 eV/atom over the close packed layer structure). This order of relative stability is also reflected in the Fermi energies: −9.89 eV (graphitic); −9.53 eV (Kagomé); −6.73 eV (close packed), as well as in the B—B Mulliken reduced overlap populations,[17] which decrease with increasing connectivity: 0.84 (graphitic, three-connected); 0.67 (Kagomé, four-connected); 0.48 (close packed, six-connected).

As they have odd numbers of electrons in their unit cells, the Kagomé and close packed boron structures would be paramagnetic. In the case of Kagomé boron, a more likely structure would be composed of anionic $(B_3^-)_n$ sheets with intercalated alkali metal cations, leading to metallic solids with the composition MB_3.

COMPARISON OF THE RELATIVE STABILITIES OF THE GRAPHITE, KAGOMÉ AND CLOSE PACKED STRUCTURES BY THE MOMENTS METHOD

The moments method[18] has been applied to Hückel-based tight binding theory very successfully by Burdett and Lee, to establish relationships between geometric and electronic structures in a variety of solids.[19] The application of the moments method to the construction of the DOS of a given structure and to the calculation of the difference in

energy between two topologically distinct structures has proved particularly useful.

In mathematical terms, the nth moment is defined as the trace of the Hückel hamiltonian matrix (**H**) to the nth power:[18]

$$Tr(\mathbf{H})^n = \Sigma_i E_i^n$$

where the summation is over all the eigenvalues (E_i) generated by **H**. In geometric terms, the nth moment (μ_n) is equivalent to the weighted sum over all closed paths of length n amongst all the orbitals of the system.[19] Moments can also be split into σ and π components if the topology of the solid permits such separation, as in, for example planar nets.

Clusters containing all walks of length 2, 3 and 4 for the graphite, Kagomé and close packed nets are depicted in Fig. 4, together with the calculated π-only 2nd, 3rd and 4th moments. Burdett and Lee have stated that the same qualitative trends are seen for $\sigma+\pi$ occupation as for π alone, except at very low and very high orbital occupations where σ-orbitals alone are being filled. A moments-based comparison of the energies of these three nets as a function of electron count is complicated by the fact that the connectivities are different. This leads directly to the calculated differences in μ_2. One-electron models can lead to wrong conclusions by overestimating the μ_2's, thereby leading to the (incorrect) prediction that the highest-coordinate net is the most stable at all electron counts.

In the cases of the Kagomé and close packed nets, there are a large number of three-rings and the inherent instability of the three-rings at high electron counts (due to the nature of μ_3) can overcome the discrepancy in μ_2 and thus give a qualitatively correct difference curve. The large difference in μ_3 for all three structures leads to the prediction of a

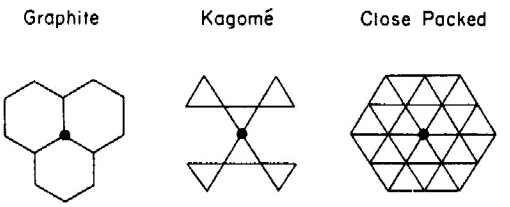

	Graphite	Kagomé	Close Packed
μ_2^π	$3\beta^2$	$4\beta^2$	$6\beta^2$
μ_3^π	0	$4\beta^3$	$12\beta^3$
μ_4^π	$15\beta^4$	$28\beta^4$	$90\beta^4$

Fig. 4. Clusters used to evaluate the 2nd, 3rd and 4th moments of the graphite, Kagomé and closed packed structures.

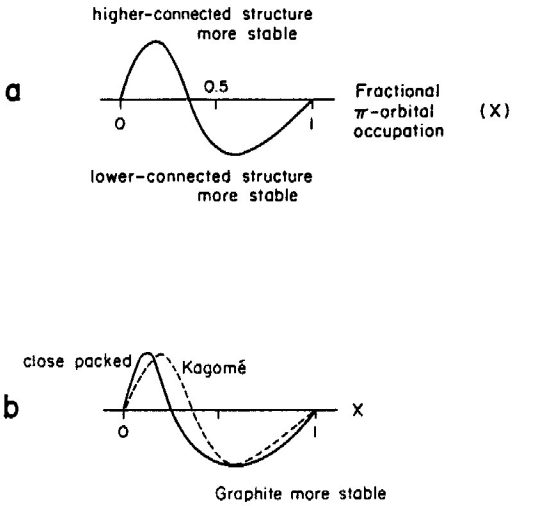

Fig. 5. Qualitative difference in energy curves as a function of the fractional occupation of the π-orbitals: (a) comparing any two of the three planar structures; (b) comparing all three structures together.

double peaked ΔE curve [see Fig. 5(a)] for graphite/Kagomé, Kagomé/close packed and close packed/graphite comparisons, with the more highly connected structure more stable until a certain band filling below the half-filled mark after which the less highly connected structure is more stable. Taken together, the close packed structure will be the most stable at very low counts, followed by the Kagomé structure and finally the graphite net is most stable, as shown schematically in Fig. 5(b). The stability of graphite for the half-filled shell is not surprising, since this is the situation for carbon. The large differences in μ_4 for the three structures may lead to extra nodes in the ΔE curves or may just create ripples on the μ_3 curve. As mentioned above, the differences in μ_2 will extend the range of stability of the more highly connected Kagomé and (especially) close packed structures to somewhat higher electron counts.

ELECTRONIC STRUCTURE OF A TRIGONALLY DISTORTED KAGOMÉ NET

In the hexagonal Laves phases ($MgZn_2$ type) the Kagomé nets of atoms (e.g. Zn) are often distorted such that the triangles alternate in size, as shown in **12**.[20] Such distortions are due to the capping of every second triangle above and below the Kagomé plane by zinc atoms, so that the capped triangles expand and the uncapped ones contract. It was decided to establish the effect of such a distortion on the π-bands of the boron Kagomé net.

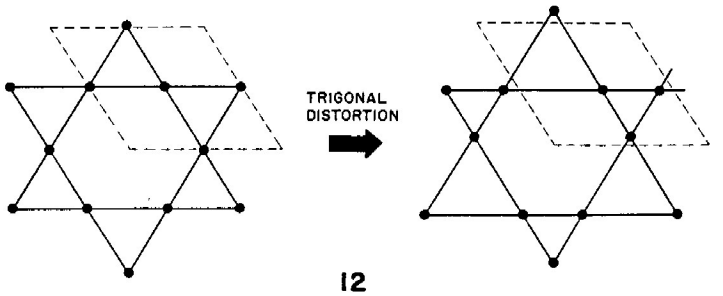

12

The B—B distances in the distorted Kagomé net are 1.70 and 1.90 Å, respectively. Since the average is 1.80 Å, the unit cell is the same size as in the undistorted case. The partial (π-only) band diagram for distorted Kagomé boron is shown in Fig. 6. The distorted Kagomé net possesses the same Bravais lattice as the undistorted net so the BZ has the same shape (**4**), though, as will be discussed below the symmetries of the special k points are different.

Comparing Fig. 6 with Fig. 1(b) reveals one very noticeable feature, namely that the lowest π-bands at K (π_1/π_2) are no longer degenerate in the distorted structure (the splitting is approximately 1 eV for the distortion indicated above). In the following paragraphs, this loss of degeneracy will be rationalized using two different, though related explanations. The first makes use of symmetry arguments while the second, more empirical but more apparent explanation, uses simple ideas related to the changing of bonding and antibonding interactions as the structure is distorted.

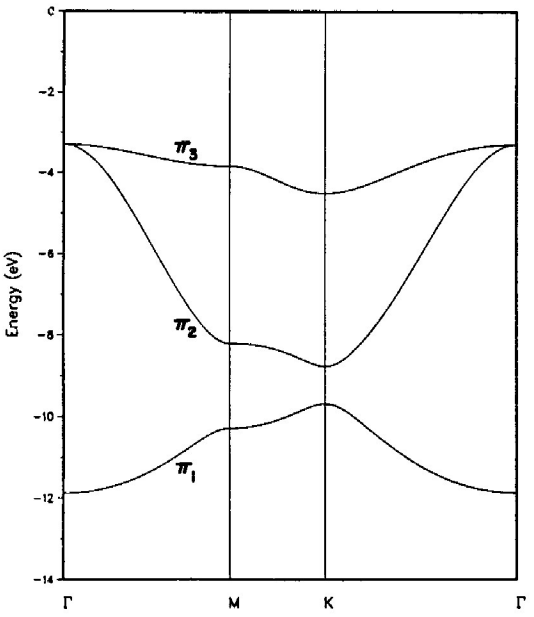

Fig. 6. π-Band diagram for boron with the trigonally distorted Kagomé structure.

The distorted Kagomé structure no longer has a six-fold axis and belongs to the plane group $p3m1$. If we include the horizontal mirror plane the distorted Kagomé net belongs to the three-dimensional space group $P\bar{6}m2$ (D^1_{3h}).[6] The symmetries of the special points in the BZ are as follows: $G_\Gamma = D_{3h}$; $G_M = C_{2v}$; $G_K = C_{3h}$ (the symmetries of the symmetry lines are: $G_\Sigma = C_{2v}$; $G_T = G_\Lambda = C_s$).[12] Thus, we expect to see some degenerate bands at Γ, but not at M. The point K is less straightforward, however. Although the point group C_{3h} does have degenerate representations (e' and e''), these representations are complex. The effect of this is that there are no degeneracies at K, but rather those bands of e' or e'' symmetry at K have their degenerate counterparts at $-K$. The character of the two components of the e (i.e. e' or e'') representations with respect to the three-fold rotation axis are ε and ε^*, where $\varepsilon = \exp(2\pi i/3)$ and, therefore $\varepsilon^* = \exp(-2\pi i/3)$. These represent phase angle changes upon C_3 rotation of 120 and 240° (−120°), respectively. Such a reversal does in fact occur as a consequence of time inversion (which is what interrelates $\pm K$).

The same lowering of symmetry and consequent loss of degeneracy at K is observed on going from graphite ($P6mmm$) to the boron nitride net ($P\bar{6}m2$) by replacing alternating carbons in the graphite structure by boron and nitrogen atoms.[21] As mentioned earlier, the Kagomé lattice is topologically related to that of graphite by the fact that the centroids of the triangles in the Kagomé net define the vertices of the graphite net. Thus the distorted Kagomé net, where alternate triangles are distinguishable, is topologically (and symmetry) related to the boron nitride structure. The loss of degeneracy between π_1 and π_2 at K on going from graphite to boron nitride can simply be explained by looking at the functional form of the crystal orbitals at this point. As shown in **9c**, π_1 and π_2 can be expressed as crystal orbitals with non-zero coefficients on either the starred or the unstarred (but not both) sets of atoms of the alternant graphite net. (The terms starred and unstarred refer to the convention of labelling every second atom of an alternant hydro-

carbon with a star, so that no two starred atoms are bonded.)[14] Upon substituting the carbon atoms by borons at the starred positions and by nitrogens at the unstarred positions the Hückel energies of the π-orbitals are simply α(B) and α(N). There is a loss of degeneracy simply because nitrogen is more electronegative than boron [i.e. α(N) is more negative than α(B)].

A similar analysis can be applied to the distortion of the Kagomé net. The π-symmetry crystal orbitals of the undistorted net, at the point K, are shown in Fig. 7. In this case the lowering in symmetry does not come about due to atom substitution (i.e. the loss of degeneracy is not due to changing α's) but rather arises out of the fact that the bond lengths are no longer constant. The Hückel β's are smaller for the longer bonds. If the central triangles of the crystal orbitals shown in Fig. 7 are contracted and the outer ones expanded, one component (labelled π_a in the figure) rises in energy because the antibonding interactions increase and the bonding ones decrease. The reverse is true for the second component (π_b) which, therefore descends in energy. Thus, the degeneracy is lifted. The π_3 crystal orbital is, however, essentially unaffected by the trigonal distortion because the increased antibonding interactions within the smaller triangles are approximately compensated by the decreased antibonding interactions within the larger triangles. To determine which of these two changes wins out it is necessary to know the change in interaction energy (whether as a Hückel β or some complex function of the overlap integral S) as a function of internuclear separation.

STRUCTURES OBTAINED BY MAKING SUBSTITUTIONS IN THE KAGOMÉ NET

As in the case of the graphite to BN "transformation", the symmetry of the Kagomé net can be lowered by substituting some of the sites.

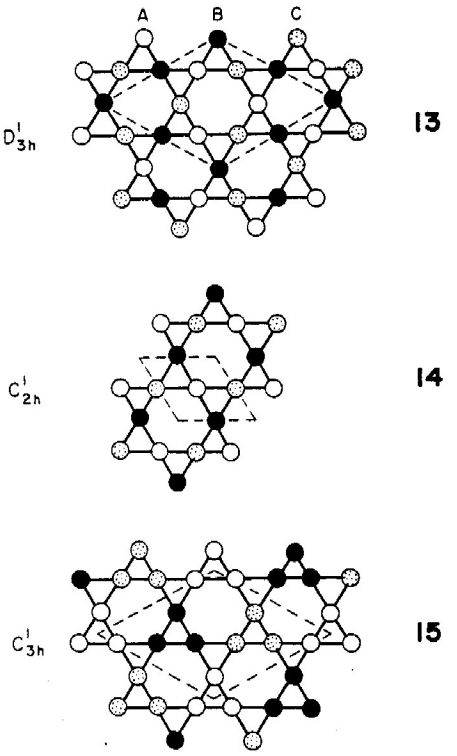

(i) *ABC substitutions*

In **13–15** are shown three derivatives of the Kagomé net, all with the stoichiometry ABC. The substitution patterns shown in **13** and **14** are three-alternant. The pattern in **13** has D^1_{3h} symmetry (as in BN) as half of the mirror planes of the Kagomé net have been lost, as well as the C_3 axes at the centre of the triangles. In contrast to the graphite/BN case, however, the substitution results in a unit cell which is three times as large as the original (i.e. nine atoms). This means that the loss of degeneracy due to lowering space group symmetry is countered by increased degeneracies due to band folding.[7c] It should be noted that this pattern is that observed for crystal orbital π_3 at K (see Fig. 2).

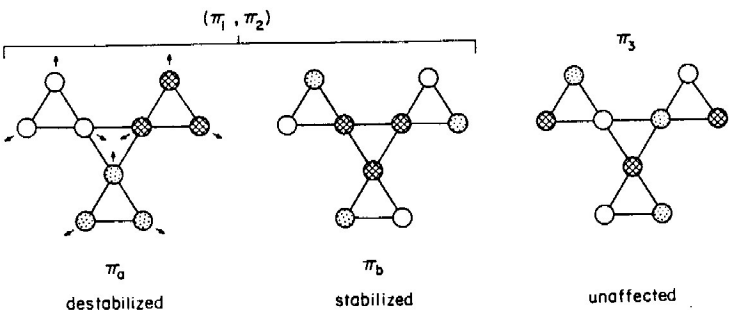

Fig. 7. Representation of the π-bands at K for the Kagomé structure, including the effect of the trigonal distortion (indicated by arrows at left) on their energies.

The substitution pattern shown in **14**, while also being three-alternant, is distinct from the first as going along straight lines of atoms in the structure the pattern is –A–B–A–B–A–; –B–C–B–C–B– and –A–C–A–C–A–, rather than –A–B–C–A–B–C– etc. This second pattern has much lower symmetry (C^1_{2h}), possessing C_2 axes (perpendicular to the net) at the atom sites and at the centres of the hexagons, with three atoms in the non-hexagonal unit cell (assuming all bond lengths are unequal). In terms of crystal orbitals, the shading of **14** is equivalent to a complex representation of one of the π_2, π_3 pair at Γ.

The substitution pattern shown in **15** is non-alternant, consisting of A_3, B_3 and C_3 triangles. Even with unequal bond lengths, three-fold symmetry is maintained at the centres of the hexagons and half of the triangles, though all vertical mirror planes and the C_6 axis have been lost. As for the first shading, the unit cell is three times the size of the Kagomé cell. This shading has the same symmetry (C^1_{3h}) as the complex representations of π_1 and π_2 at K (see Fig. 2).

(ii) *AB_2 substitutions*

Replacing atom type C by B in the pattern shown in **13** yields the AB_2 structure shown in **16**. The

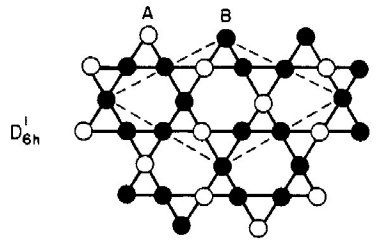

16

symmetry is D^1_{6h} once more, but with a nine-atom (A_3B_6) unit cell. It is intriguing to think of this pattern as representing a possible MC_2 solid, with planar C_6 rings having each edge coordinated to a metal atom (see **17**). The possibility of metal–metal bonding also exists.

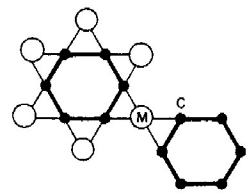

17

A similar substitution in the ABC net of **14** leads to an AB_2 net with parallel chains of B atoms coordinated to A atoms, as shown in **18**. A possible realization of this pattern is the metal–poly-

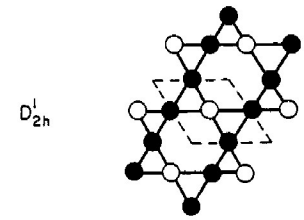

18

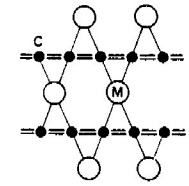

19

cumulene MC_2 structure shown in **19**. The symmetry is once again increased on going from ABC to AB_2, with the generation of vertical mirror planes leading to D^1_{2h} symmetry.

SUMMARY

The electronic band structure characteristic of a Kagomé net of boron atoms has been determined and compared with topologically related graphite and close packed (triangular) nets. The dispersion of the bands in these structures has been rationalized from a simple Hückel viewpoint and a method for determining the interaction between atomic orbitals with complex coefficients has been developed. This, together with an analysis of the topological relationships between the three nets has facilitated their comparison and enabled explanations to be constructed. The application of a moments analysis has shown how the relative stabilities of the three structures may vary with electron count. The symmetry reasons for the loss of band degeneracy at K upon trigonally distorting the Kagomé net, have also been rationalized. Finally, ABC and AB_2 substitution patterns have been presented and the effect of substitution on the symmetries of the net discussed.

Acknowledgements—The initial impetus for this work came from correspondence with Dr A. K. Cheetham concerning the bonding in Laves phase intermetallics (see ref. 5). The authors also wish to thank Dr P. A. Cox for helpful discussions, Jane Jorgensen and Elizabeth Fields for their expert drawings and Edith Chan for help in plotting one of the band pictures. R.L.J. is grateful to

the Science and Engineering Council of Great Britain for the award of a NATO postdoctoral fellowship. The research was supported by the National Science Foundation through research grants CHE84064119 and DMR84722702.

REFERENCES

1. (a) A. F. Wells, *Three-dimensional Nets and Polyhedra*. John Wiley, New York (1977); (b) W. B. Pearson, *The Crystal Chemistry and Physics of Metals and Alloys*, Ch. 2. John Wiley, New York (1972).
2. (a) W. B. Pearson, *The Crystal Chemistry and Physics of Metals and Alloys*, Ch. 12. John Wiley, New York (1972); (b) F. Laves, in *Intermetallic Compounds* (Edited by J. H. Westbrook), p. 129. Wiley, New York (1967); (c) J. H. Wernick, *ibid.*, p. 197.
3. For a discussion of physical properties and further references see: B. M. Klein, W. E. Pickett, D. A. Papaconstantopolous and L. L. Boyer, *Phys. Rev. B* 1983, **27**, 6721.
4. (a) S. Samson, in *Structural Chemistry and Molecular Biology* (Edited by A. Rich and N. Davidson), p. 687. Freeman, San Francisco (1968); (b) K. Girgis, in *Physical Metallurgy* (Edited by R. W. Cahn and P. Haasen), 3rd edn, Ch. 5. Elsevier, Amsterdam (1983).
5. R. L. Johnston and R. Hoffmann, manuscript in preparation.
6 *International Tables for Crystallography. Vol. A: Space-group Symmetry* (Edited by T. Hahn). Reidel, Dordrecht, Netherlands (1983).
7. (a) R. Hoffmann, *J. Chem. Phys.* 1963, **64**, 1397; (b) M.-H. Whangbo and R. Hoffmann, *J. Am. Chem. Soc.* 1978, **100**, 6093; (c) R. Hoffmann, *Angew. Chem. Int. Edn Engl.* 1987, **26**, 846; *Angew. Chem.* 1987, **99**, 871; (d) A. B. Anderson and R. Hoffmann, *J. Chem. Phys.* 1974, **60**, 4271; (e) R. Ramirez and M. C. Böhm, *Int. J. Quantum Chem.* 1986, **30**, 391.
8. J. Donohue, *The Structure of the Elements*, 2nd edn. John Wiley, New York (1974).
9. (a) W. N. Lipscomb, *Boron Hydrides*. Benjamin, New York (1963); (b) E. L. Muetterties (Ed.), *Boron Hydride Chemistry*. Academic Press, New York (1975).
10. (a) L. A. Paquette, *Accts Chem. Res.* 1971, **4**, 280; (b) R. J. Ternansky, D. W. Balogh and L. A. Paquette, *J. Am. Chem. Soc.* 1982, **104**, 4503.
11. (a) K. Wade, *Adv. Inorg. Chem. Radiochem.* 1976, **18**, 1; (b) R. B. King and D. H. Rouvray, *J. Am. Chem. Soc.* 1977, **99**, 7834.
12. C. J. Bradley and A. P. Cracknell, *The Mathematical Theory of Symmetry in Solids*. Clarendon Press, Oxford, U.K. (1972).
13. E. Heilbronner and H. Bock, *The HMO-model and its Application*. John Wiley, New York (1976).
14. See, for example: D. M. P. Mingos and Z. Lin, *New J. Chem.* 1988, **12**, 787.
15. R. L. Johnston, Z. Lin and D. M. P. Mingos, *New J. Chem.* 1989, **13**, 33.
16. P. A. Cox, *The Electronic Structure and Chemistry of Solids*, Ch. 4. Oxford University Press, Oxford, U.K. (1987).
17. T. A. Albright, J. K. Burdett and M.-H. Whangbo, *Orbital Interactions in Chemistry*, Ch. 2. John Wiley, New York (1985).
18. J. P. Gaspard and F. Cyrot-Lackmann, *J. Phys. C* 1973, **6**, 3077 and refs therein.
19. (a) J. K. Burdett and S. Lee, *J. Am. Chem. Soc.* 1985, **107**, 3050; (b) J. K. Burdett and S. Lee, *J. Am. Chem. Soc.* 1985, **107**, 3063.
20. (a) T. Ohba, Y. Kitano and Y. Komura, *Acta Cryst. (C)* 1980, **40**, 1; (b) M. M. J. de Almeida, M. M. R. Costa, L. Alte da Veiga, L. R. Andrade and A. Matos Beja, *Portg. Phys.* 1980, **11**, 219; (c) M. M. R. Costa and M. J. M. de Almeida, *Portg. Phys.* 1986, **17**, 173.
21. (a) E. Doni and G. Pastori Parravicini, *Nuevo Cimento* 1969, **64B**, 117; (b) J. Zupan, *Phys. Rev. B* 1972, **6**, 2477; (c) A. Zungar, A. Katzir and A. Halperin, *Phys. Rev. B* 1976, **13**, 5560.